Springer

KSME

Journal of Mechanical Science and Technology 33 (10) (2019) 5073~5083
www.springerlink.com/content/1738-494x(Print)/1976-3824(Online)
DOI 10.1007/s12206-019-0946-1

Experimental study on ignition characteristic of gasoline-biodiesel blended fuel in a constant-volume chamber †

Dinh Nam Vu[1] and Ocktaeck Lim[2,*]

[1]*Graduate School of Mechanical Engineering, University of Ulsan, Ulsan 44610, Korea*
[2]*School of Mechanical Engineering, University of Ulsan, Ulsan 44610, Korea*

(Manuscript Received March 26, 2019; Revised June 16, 2019; Accepted July 24, 2019)

Abstract

A detailed experimental study on gasoline biodiesel fuel (GB) blends was conducted to investigate its ignition and combustion characteristics under low-temperature range using an optically accessible constant volume combustion chamber (CVCC). The fuel samples were four GB blends including GB20, GB40, GB60 and GB80 corresponding to 20 %, 40 %, 60 %, and 80 % volumetric biodiesel respectively, neat gasoline, and neat biodiesel. Fuel samples were injected into the CVCC to combust using a single-hole research-grade injector. Natural soot luminous images from the combustible flame were captured by a CMOS camera to determine the ignition delay and the flame lift-off length. The ignition delay was also obtained by analyzing pressure traces from a high-frequency piezoelectric pressure transducer. The results regarding the ignition process for the pressure-based and luminosity-based ignition delays showed that both approaches presented similar tendencies. However, the pressure-based ignition delay is always a little longer than the luminosity-based ignition delay. The difference between the two definitions of ignition delay tends to decrease with the longer ignition delay or the enhanced mixing, and vice versa. As lower 60 % biodiesel fractions, the increase of biodiesel significantly reduced ignition delay and produced a lower maximum peak of heat release rate. The combustion characteristic of blend with a higher 60 % biodiesel is almost similar to pure biodiesel. In general, lift-off length lengthens with an increase in biodiesel because of its high viscosity and high surface tension. However, for the 750 K case, the lift-off length decreases due to a rapidly reduced ignition delay with the increase in biodiesel fraction (less than 60 % biodiesel). Based on experimental data, the moderate biodiesel addition (less than 20 %) can improve the ability of cold-engine starting, also solve engine misfire under low-load-condition operation due to its flammability while maintaining advantages of gasoline with great volatility and high ignition delay which significantly enhance the mixture formation process.

Keywords: Gasoline biodiesel blend; Ignition delay time; Low-temperature combustion; Flame lift-off length; Cold-engine starting

1. Introduction

Over their hundred-year development, compression ignition (CI) engines have evolved into one of the world's most capable and reliable forms of motive power for transportation due to high fuel efficiency and high-power output [1-4]. To meet stringent emission standards and satisfy the demand for decreasing fuel consumption, the CI engines need to continue to adapt the fuel consumption and improve to reduce emissions while retaining engine performance and power output. Emissions of nitrogen oxides (NOx), total hydrocarbons (THC), carbon monoxide (CO), particulate matter (PM), and greenhouse gases have been a severe problem that needs to be solved for CI engines [5, 6]. Hence, near-term solutions, including diesel oxidation catalysts, diesel particulate filters, selective catalytic reduction, and lean NOx trap regeneration, have been used to remove the emissions [7]. High cost is a big barrier to the after-treatment techniques to apply commonly in IC engines. Additionally, diversifying combustion methods and using alternative fuel are long-term solutions to reduce pollutant emissions.

One of the long-term solutions, gasoline fuel has been used for CI engines to increase engine efficiency and significantly reduce hazardous emissions such as NOx and soot emission. The prospective combustion method is referred to as the gasoline compression ignition (GCI) since it relies on gasoline fuel to reach its auto-ignition limitation in CI engines. The GCI utilizes the advantage of low-temperature combustion to stay out of the high soot and NOx formation zones while increasing thermal efficiency such that it approaches that of a diesel engine [8-10]. However, the future challenge of GCI engines is somewhat questionable due to its limitation in the low load operating range. Gasoline is highly volatile and shows poor self-ignition. Therefore, it helps to extend the air-fuel mixing time to reach a homogeneous charge compression ignition

*Corresponding author. Tel.: +82 522592852, Fax.: +82 522591680
E-mail address: otlim@ulsan.ac.kr
† Recommended by Associate Editor Jeong Park

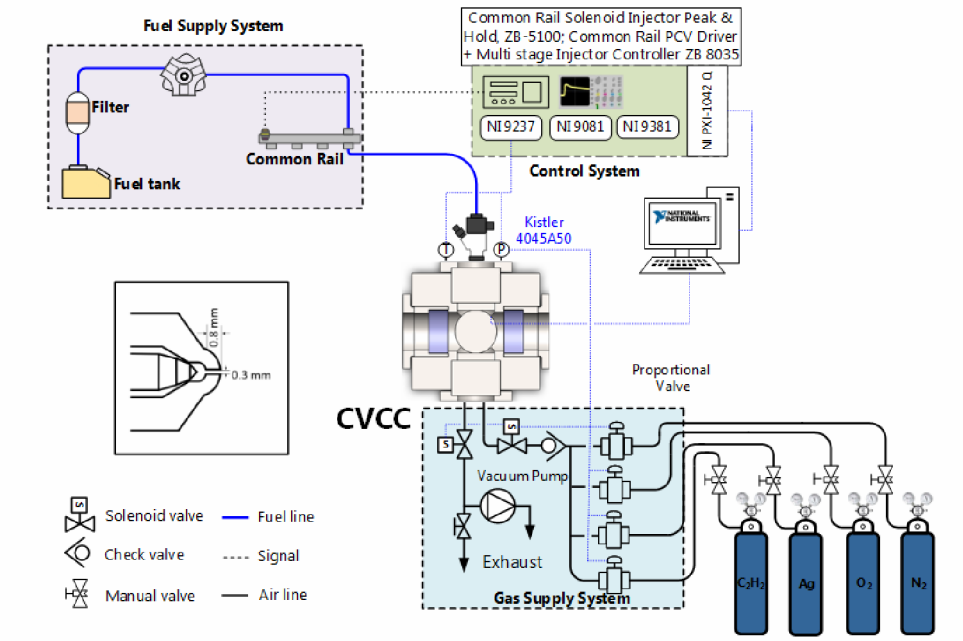

Fig. 1. Scheme of the constant-volume combustion chamber performed in this work.

mode (HCCI). But the problem is that it is hard to combust/ignite at low-temperature conditions such as cold-start, low-load engine conditions. To solve these problems, the fuel must be highly chemically reactive, and so diesel [11] or biodiesel [12] is added and mixed with the gasoline to improve its ignition characteristics.

For example, Hanson et al. [13] used reactivity controlled compression ignition (RCCI) approach for gasoline-diesel dual fuel to reduce NOx and PM emissions, while maintaining high efficiency using the KIVA 3V software combining with experiment. The authors found that brake thermal efficiency was improved from 37 % to 40 %, increasing combustion efficiency to 96 %, and low NOx and PM emissions. Yang et al. [14] carried out numerical simulation and experiments for gasoline-diesel fuel under two different combustion strategies: Highly premixed charge combustion and low-temperature combustion. The authors found that low-temperature combustion mode leads to a fast heat release rate and a high maximum pressure rise rate because of the coupling combustion reaction of gasoline and diesel taking place in regions with higher fuel concentration. The early-highly premixed charge combustion reduces NOx and soot emissions due to the avoidance of high equivalence ratio and high-temperature region in the combustion chamber. Curran et al. [15] experimented the fuel blending of gasoline with diesel controlled the combustion phasing to improve efficiency and emission. The authors found that the controllability of cylinder-to-cylinder balancing is the most important determinant for obtaining stable combustion and high thermal efficiency. The study also showed an increase in thermal efficiency, and an approximate 90 % reduction in NOx and PM and brake thermal efficiency of 33.5 %. Adams et al. [16] used gasoline blending with biodiesel content at 5 % and 10 % levels to extend to the low load conditions, enhance the combustion stability, and reduce the intake temperature requirement. Yanu et al. [17, 18] studied the change of injection timing, exhaust gas recirculation (EGR), and different intake air temperatures to gain an optimum region for GB blended fuels with 5 %, 10 %, 15 %, and 20 % biodiesel. The research showed that the thermal efficiency archives approximately 92 %; also, THC and CO emissions diminished 50 % compared to diesel. Use of biodiesel fuel blending with gasoline is a possible way to extend GCI combustion to low load condition due to its high ignitability. Moreover, biodiesel fuel is an alternative fuel that can be used in regular diesel engines without making any changes to the engines and is currently of great interest and an important research subject for reducing soot formation, harmful gas emissions, and greenhouse gas. It is a clean and renewable energy source with superior lubricity, free of sulfur, and free of aromatics. Biodiesel can synthesize from abundant feedstocks, which drive to various chemical structures and contain oxygen in biodiesel molecules resulting in the ability to complete combustion [19-21]. In such situation of fossil fuels resources depletion, biodiesel fuel has attracted more and more attention.

Although many optical investigations have conducted for diesel fuel, there are no experimental measurements for GB blended fuels. Therefore, the CVCC with an optically accessible ability was used to investigate GB blends on the aspect of ignition delay and lift-off length in this work. Natural luminous soot emission images and pressure profiles were used to determine the ignition behavior and lift-off length for GB blends under low-temperature range representing cold-start and low-load engine conditions where pure gasoline is diffi-

Table 1. Gasoline-biodiesel blended fuel compositions (vol%).

Fuel	Component (vol%)
G	Gasoline 100 %
GB20	Gasoline 80 % + biodiesel 20 %
GB40	Gasoline 60 % + biodiesel 40 %
GB60	Gasoline 40 % + biodiesel 60 %
GB80	Gasoline 20 % + biodiesel 80 %
B	Biodiesel 100 %

cult to burn because of extremely high ignition delay, causing the misfiring. Both parameters play an essential role in combustion spray, which governs the engine operating range as well as engine efficiency and soot emission. The ignition delay affects the degree of fuel atomization and the amount of air entrainment into fuel spray to create an initial mixture for spray combustion [11, 22]. Besides, the lift-off region is a critical zone where is bounded by the injector tip and the high frame region wherein the air entrainment into the jet takes place [23, 24]. We have confidence that these experimental results will help promote the application of GB blends in low-temperature range and spray combustion modeling in the future.

2. Experimental setup

2.1 Constant-volume combustion chamber

Fig. 1 presents the CVCC including a gas supply system, a chamber body, the intake and exhaust lines, a fuel system, a fan, and a National Instruments (NI) computer. The chamber was added quartz windows to allow the optical investigation of ignition delay and lift-off length via natural luminous soot emission. The premixed charge was composed of acetylene (C_2H_2), argon (Ar), oxygen (O_2), and nitrogen (N_2) filled sequentially to reach the desired partial pressure targets. A self-written Matlab program controls proportional control valves to fill the premixed charge and a fan to mix the premixed charge homogeneously before the spark plug ignites them. The fuel system is a common-rail direct fuel injection system and can feature a high-pressure of up to 1600 bar. Eight heater elements with a PID temperature controller maintain wall temperature (353 K) to ensure complete combustion of the premixed charge gases. A high-frequency pressure sensor coupled with a charge amplifier measures dynamic pressure. The high-pressure solenoid valves were used to exhaust the hot gaseous product. On the other hand, the chamber was quickly and automatically evacuated using a vacuum pump to remove any remaining gas to ensure the chamber is empty for the next experiment.

2.2 Fuel preparation

This work aims to investigate the effects of difference gasoline-biodiesel blending ratio on its combustion spray. Therefore, a wide blending range of fuel samples, including GB20, GB40, GB60, and GB80 (biodiesel fractions of 20 %, 40 %, 60 % and 80 % by volume respectively as listed in Table 1)

Table 2. Chemical composition and properties of gasoline.

Specification name	Value	Test method
RON	94	KS M 2039
Sulphur, max (ppm)	10	KS M 2027
Lead, max (g/l)	0.013	KS M 2402
Benzene, max (vol. %)	0.7	ASTM D6296
Aromatics, max (vol. %)	24	ASTM D1319
Olefins, max (vol. %)	18	ASTM D1319
RVP @ 37.8 C, max (kPa)	60c	KS M ISO 3007
Oxygen, min (wt. %)	0.5(s) / 1(w)	KS M 2408 ASTM D4815
Oxygen, max (wt. %)	2.3	
Methanol, max (vol. %)	0.1	
Distillation		
T_{10}, max (C)	70	KS M ISO 3405
T_{50}, max (C)	125	
T_{90}, max (C)	170	
FBP, max (C)	225	

Table 3. Chemical composition and properties of biodiesel.

Specification name	Value	Test method
Ester content, mass%	97.8	KS M 2413
Flash point, °C	190	KS M 2010
Viscosity at 40 °C, mm^2/s	4.4	KS M 2014
Carbon residue, wt%	0.01	KS M ISO 10375
Sulfur content, mg/kg	1	KS M 2027
Ash, wt%	0.001	KS M ISO 6245
Copper strip corrosion (3h at 50 °C)	1A	KS M 2411
Density at 15 °C, kg/m^3	878	KS M 2411
Water content, %	0.04	KS M ISO 12937
Total contaminant, mg/kg	7	EN 12662
Acid value, mg KOH/g	0.2	KS M ISO 6245
Total glycerol, mass%	0.16	KS M 2412
Monoglyceride, mass%	0.47	KS M 2412
Diglycereol, mass%	0.17	KS M 2412
Triglycereol, mass%	0	KS M 2412
Free glycerol, mass%	0.0132	KS M 2412
Oxidation stability, 100 °C, h	15	EN 14112
Methanol content, mass%	0.01	EN 14110
Metal (mg/kg) Na + K	LT1	EN 14108, 14,109
Ca + Mg	LT1	Pr EN 14538
Phosphorous content, mg/kg	LT1	EN 14107
Color (ASTM)	1	ASTM D1500
Pour point, °C	0	KS M 2016
CFPP, °C	−2	KS M 2411
Appearance	Clear	Naked eyes

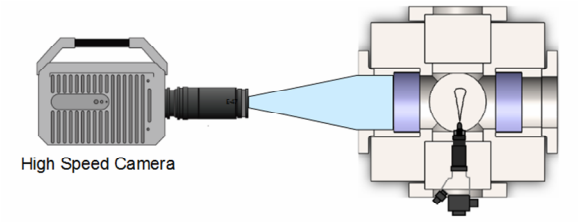

Fig. 2. The optical set up for the natural light emission visualization.

was created, then burn in the CVCC, and compare with the combustion of pure gasoline and pure biodiesel. The biodiesel was derived from soybeans, and the gasoline comes from the S-oil network, South Korea. All fuels were stored in a controlled temperature and humidity device. The homogeneous GB fuels were prepared by a rotary mixing/shaking process for 10 min to avoid phase separation and crystalline colloids. The chemical composition and properties of gasoline and biodiesel following the Korean standard had very different properties as exhibited in Tables 2 and 3 [25].

2.3 Optical arrangement

Fig. 2 presents the setup for observation of the natural light emission from spray combustion of gasoline-biodiesel blended fuels. A high-speed CMOS camera (Photron SA3) with a Nikkor lens was used to obtain the natural soot luminosity imaging at 512×128 pixels and rate of 20000 frames/s, which corresponds to a 40 μs increment for each image. The injected signal from the injector triggers the camera to start recording the set of combustion images.

2.4 Definition of ignition delay

The time interval from the start of injection to the start of combustion was defined as the ignition delay. The start of injection is the time at which the fuel appeared at the injector tip, and the injection began. The start of injection was determined from the injected current signal, which was given to trigger the injector. All injectors have a delay due to the inertia of the needle valve and spring assembly. The injection delay was determined through macroscopic spray images in Shubra's research [25]. The start of combustion was determined via two different techniques, i.e., pressure-based ignition delay and the luminosity-based ignition delay.

The pressure ignition delay was determined by tracking the combustion pressure. The starting point of combustion was designated to be the point where the pressure starts to depart from a slight initial drop because of heat release from the combustion process. Before this point, adiabatic mixing between fuel and ambient gas takes place. In this process, the fuel is atomized, vaporized, mixed in the chamber and slightly decreases the bulk ambient gas temperature. This definition produces the smallest difference between luminous and pressure ignition delay [26] as illustrated in Fig. 3.

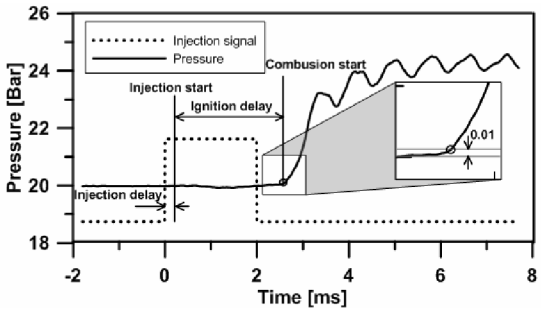

Fig. 3. Definition of the ignition delay based on pressure trace.

The luminous ignition delay is the elapsed time from the start of injection to the time of high-temperature flame, which based on the light of the flame from the combustion of fuel. Set of combustion images captured by the CMSO camera is processed to determine the start of combustion. The image undergoes the image processing in order to extract ignition information from it. The start of combustion is timing when the high-temperature flame is getting started with high chemiluminescence and heat release. The high-temperature flame generates an intense and stable radiation called the high-temperature luminosity. The 50 % digital level (125) of this value was chosen as the thresholding of high-temperature flame segmentation. This is recommended by Engine Combustion Network (ECN) guidelines and adopted in previous studies [27-29]. The threshold is significantly higher than luminosity emission from low/intermediate temperature chemistries of gasoline which generated before the main ignition stage. In this stage, the temperature can increase during the autoignition, and hence, a tiny fraction of soot could be generated. The threshold has to ensure removing it in the image processing. The threshold is also significantly lower than high high-temperature flame. The appearance of the first high-temperature flame is at 0.85 ms reflects the start of combustion. The approach has demonstrated to correspond with results from broadband chemiluminescence images, and the high-temperature flame is bounded in the red line, as shown in Fig. 4.

2.5 Evaluation of the flame lift-off length

Immediately after the fuel ignites, spray flame will locate in a relatively stabilized position slightly away from an injector orifice. The distance is called flame lift-off length, which was measured through natural light emission by soot emission, as presented in Fig. 5. There are many factors affecting lift-off length, such as engine operating conditions, fuel properties, and injection characteristics. The lift-off length is an important factor of the spray combustion process that affects the chemical reaction directly, thus governing pollutant emission. It is the driving parameter to identify the combustion rate and soot formation and determine the amount of fuel-air premixing before combustion [30, 31]. A high-speed ICCD camera com-

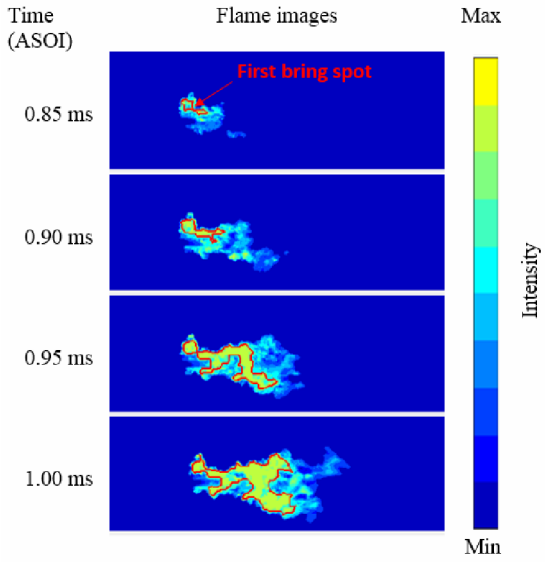

Fig. 4. Images of combustion development sequence.

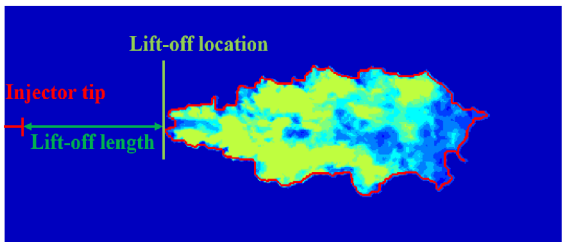

Fig. 5. Lift-off length measurement from the natural soot emission image.

bined with optical bandpass filters was utilized to obtain the emission of light from OH radicals to determine the lift-off length [28, 32]. However, the test equipment for this measurement requires a complicated optical setup. In some cases, there can be confusion due to the release of OH radicals from other sources. In this work, the lift-off length is measured through natural light emission by soot emission. It is much easier and simpler to perform than using OH radicals. The fundamental premise of the technique is to clear the low intensity emission/reflection of the liquid/vapor core, and background noise. The Gaussian method is utilized to process the flame images and presented in detail in next section.

2.6 Image processing

Image processing is an important step for detecting the bright spot in the combustion images in this study. The computer algorithms used to separate frame and background are based on the criteria of thresholding, image segmentation, and morphological filtering. In general terms, the background slightly changed during the combustion process due to the brightness of the flame. Therefore, the Gaussian method was applied to detect frames on the image background. The background detector required a certain number of video frames to initialize the Gaussian mixture model [33]. This analysis uses the first 30 frames to initialize the Gaussian modes in the mixture model. However, the Gaussian method to split the image into the foreground and background often contains noise. The morphological structuring element was adopted as the filtering technique to reject the noise blobs and to fill gaps in the detected objects [34]. A further noise removal technique was added to clear small spots that have a size of lesser than 25 Pixels. The image was then converted to the intensity picture with the minimum and maximum intensity values. The image processing was coded by Matlab software to automatically obtain combustion flame in the natural soot luminous image video captured by the CMOS camera [35]. The area of the high-temperature flame is highlighted and zoned by the red line using the ignition threshold as the previous discussion. Addition, the flame contour automatically determined to measure the flame lift-off length. The natural light emission visualization setup and image processing scheme were unchanged to ensure repeatability and accuracy.

Table 4. Experimental conditions of the GB fuels for ignition and lift-off length measurement.

Parameters	Value
Fuel type	G, GB20, GB40, GB60, GB80, B
Injection pressure (bar)	400
Ambient gas density (kg/m^3)	10
Orifice diameter (mm)	0.30
Injector type	Bosch CRIN 2
Injection duration (μs)	5000
Chamber body temperature (K)	353
Injector nozzle type	Single hole SAC
Fuel temperature	318
Frame rate (frame/sec)	20000 frames/second
Image resolution	512x128 pixels
Premixed gas reactants (%)	21O_2, 7.6CO_2, 3.8H_2O, 65.3N_2, 2Ar
Ambient temperature (K)	750-900

2.7 Test conditions

The CVCC is an optical efficiency investigation tool for spray combustion by generating the target experimental conditions from the chemical heating process [25, 36]. The pre-filled diluted combustible mixture, including C_2H_2, Ar, N_2, and O_2, is ignited to generate the high pressure and temperature under 10 kg/m^3 density and then lets these cool down for a relatively long period to meet the desired conditions covering the range of 750 K - 900 K where the gasoline has a long ignition delay, leading to the misfiring. Fuel samples are injected to determine the ignition delay and the flame lift-off length at 400 bar injection. The oxygen concentration is selected to be 21 %, which is an air simulated oxidizer for the primary combustion in internal combustion engines. Table 4 lists the experimental conditions and all other relevant pa-

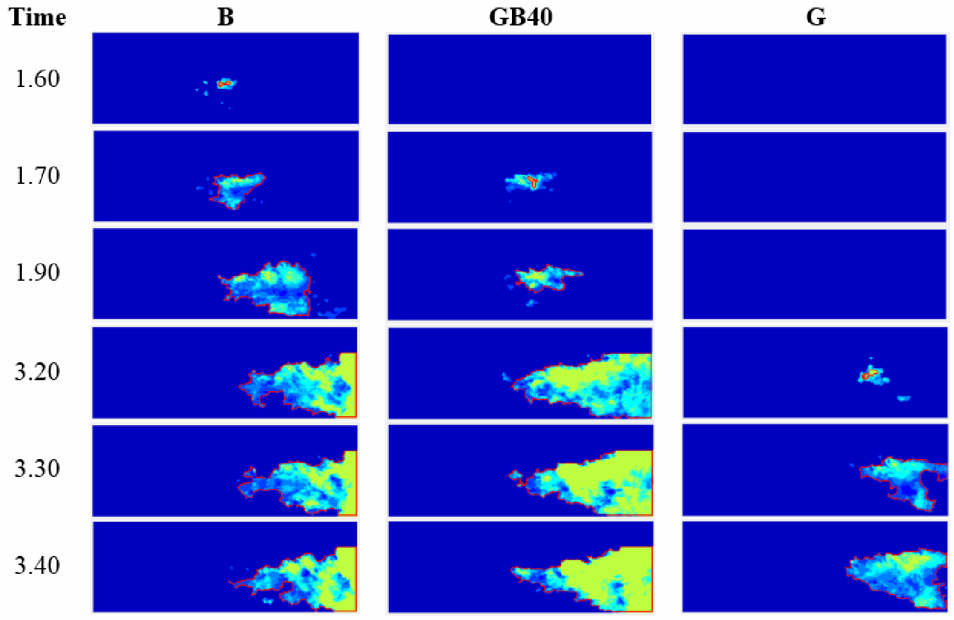

Fig. 6. Time sequence of flame images for biodiesel, GB40 blend, and gasoline under 750 K temperature, 21 % oxygen content, and 10 kg/m^3 density.

rameters. Every experiment was implemented at least ten times for each operating condition to obtain good average results. The standard deviation formulas were used to calculate the error at each tested condition for every fuel samples. Pressure data was recorded for 1s at 100000 samples per second and automatically smoothed via the Savitzky-Golay method using a ten-point average.

3. Results

3.1 Ignition delay

The focus of this section is to measure the ignition delay of the GB blends via two different methods referred to as pressure-based and luminous-based ignition delay. As discussed earlier, the natural soot luminous emission images were employed to achieve the high-temperature ignition for different gasoline biodiesel blended fuels under low-temperature conditions [26, 37, 38]. Fig. 6 manifests the typical sequences of combustion images for three fuel samples at an ambient gas temperature of 750 K, an oxygen concentration of 21 %, and a density of 10 kg/m^3. The displayed sequence begins at the start of combustion of biodiesel and ends slightly after the start of combustion of gasoline. The time-resolved image sequences help to easily visualize the ignition process and receive the ignition information. The area bounded in the red line is to emphasize the high-temperature reactivity zone. The difference in the GB blend ratio has a notable influence on ignition in particular conditions. The first bright spots appeared at 1.6, 1.7 and 3.2 ms for biodiesel, GB40 and, gasoline, respectively. The occurrence of the first bright spot signalizes the start of the combustion, and it advanced with an increase of biodiesel concentration.

Fig. 7 demonstrates the development of global pressure and heat release rate (HRR) of different GB ratios for two typical conditions. The global gas pressure is calculated by subtracting the pressure at the injection timing from the pressure measured by the pressure sensor. Shortly after fuel injection, the in-chamber pressure has a slight dip due to heat loss by cold fuel in the area of the non-reacting spray. The phenomenon can be demonstrated evidently through the appearance of a negative heat release rate after the fuel injection timing. The pressure showed a downtrend while the biodiesel concentration increases because of lower heating value for blended fuel with a higher biodiesel ratio. The decrease of input energy results in a reduction of total heat release, thus reducing the maximum global pressure. The difference in combustion phasing can be observed more clearly while biodiesel content is lower than 60 % due to the notable decrease of chemical delay. The advance in combustion phasing has a cause from the biodiesel component, which has a higher value of the cetane number compared to pure gasoline. The GB blend with a higher biodiesel content reduced the chemical delay, leading to the advanced combustion phasing. Pure gasoline has a RON (research octane number) and MON (motor octane number) that cause the most prolonged ignition delay; hence, it retarded the combustion phasing. For the 750 K case, biodiesel addition remarkably advanced the combustion phasing; it proved its potential to assist the cold-engine starting and solve misfiring under low-engine load. However, over 60 % biodiesel ratio the combustion phasing is not different so much. The increase of biodiesel content even retards combustion phasing in 900 K case. Moreover, the gasoline exhibited a maximum peak of HER because of the extension of the mixing process that leads to a larger mass of air and fuel prepared prior to the start of combustion. The opposite side, biodiesel showed the minimum peak of HRR, and the heat release rate

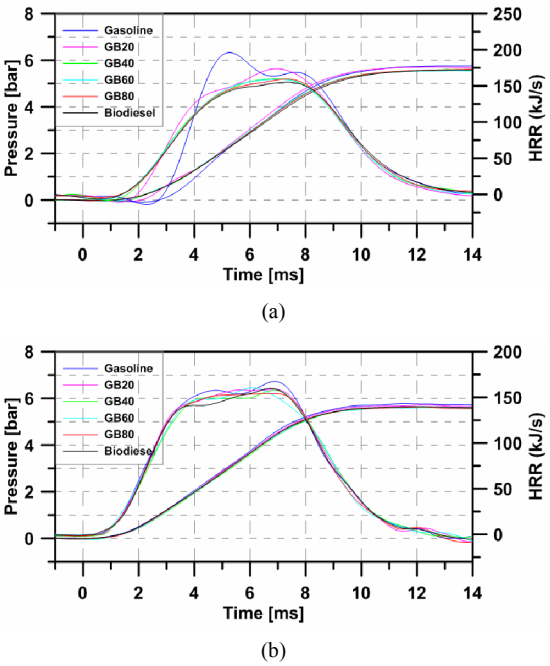

Fig. 7. Pressure and HRR for GB blends, biodiesel, and gasoline at two ambient temperatures: (a) 750 K; (b) 900 K.

curve is relatively flat and smooth. The GB60 and GB80 have similar behavior like biodiesel in both pressure profile and HRR curve.

The results showed that the fuel blend having a lower biodiesel fraction burns with a shorter duration of combustion in all tested conditions in comparison to pure biodiesel. It implies that its combustion characteristic gets more resembling the Otto cycle, thus guarding higher-engine efficiency following engine combustion network guidelines. Besides, the longer ignition delay obtained from fuel blend with lower biodiesel will enhance the fuel evaporation to make leaner air-fuel combustion, therefore diminishes soot formation. For these reasons, gasoline mixing with moderate biodiesel owns the great potential to obtain high efficiency and low emission because of maintaining advantages of gasoline. The GB blend with small biodiesel (less than 20 %) will meaningfully extend the engine operating range to low-load conditions while retaining the high thermal efficiency and low emission.

Fig. 8 presents average ignition delays and error values versus biodiesel fraction under three ambient gas temperatures (750 K, 800 K, and 900 K) for both the pressure and luminous methods. The error values which were calculated using standard deviation formulas point out total absolute uncertainty. The experimental results showed similar trends in ignition delay for both techniques. However, the pressure-based ignition delay is always a little longer relative to the luminous ignition delay. This difference between the two definitions of ignition delay is almost identical to other studies in CI engines. The reason for the difference is that a small amount of fuel

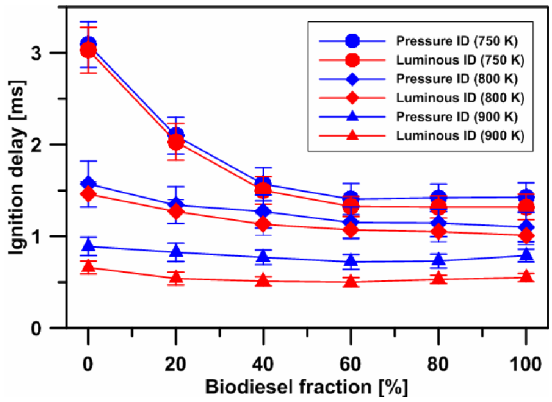

Fig. 8. Ignition delay under different temperature of 750 K, 800 K and 900 K temperature, 21 % oxygen content, and 10 kg/m^3 density.

first reaches the limitation reaction conditions and then produces a first little bright spot, which generates a small amount of energy. This energy is not enough to increase the pressure. A small amount of time is required for the heat to compensate for a slight pressure drop due to the adiabatic mixing process, and then reach the pressure sensor.

The difference between the two definitions becomes more severe as the ambient temperature increases. As the ambient temperature increases from 750 K to 900 K, the average value of difference increases from 0.08 to 0.23 ms. The reason for the bigger difference is the shorter time for atomization, vaporization, and mixing with air. Therefore, the amount of air-fuel mixture that reaches a self-ignition temperature is smaller. The smaller amount of air-fuel mixture before the start of combustion causes a decrease in the rate of expansion of the flame. In contrast, the longer ignition delay causes a higher concentration of oxygen at the fuel-rich combustion zone, which accelerates oxidation reactions and speeds up the flame speed. The time required for generating enough energy to reach the pressure sensor is shorter. Conversely, the luminous ignition delay considered from the bright flame is independent the flame speed. For all these reasons above, the difference between the two definitions can increase or decrease depending on the mixing process and the period of ignition delay.

The ambient gas temperature effect on the difference of two definitions are also clearly demonstrated through time-sequenced flame footages as shown in Fig. 9 for the spray combustion of GB20 under different temperatures (750 K, 800 K, and 900 K). For the better collation of different ambient temperatures, the ignition delay was ignored to make all sequences begin at the same time (the start of the combustion). The time scale of each spray combustion image inscribes at the left column, which signifies the different evolutions of spray combustion at that specific time after the start of ignition. For 750 K the development of contour plots of flame (rate of expansion of the flame in a combustion reaction) is faster than the others during the spray combustion process, thus reducing the time requirement to reach the pressure sensor. In this case, the difference between the two definitions is smaller than

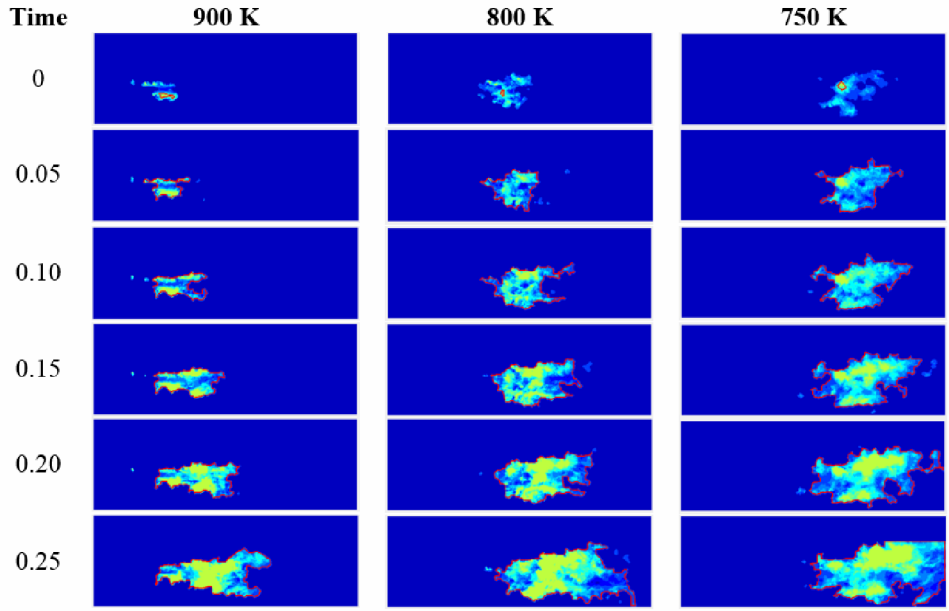

Fig. 9. Development of flame for GB20 blend under different ambient temperature (750 K, 800 K, and 900 K), oxygen concentrations of 21 % condition, and density of 10 kg/m^3.

800 K and 900 K cases.

Generally, the ignition delay decreases with increase biodiesel content due to increasing of cetane number. But for an ambient temperature of 900 K, first, the increase in biodiesel decreases the ignition delay due to its higher cetane number. However, the content of biodiesel is higher than 60 %; the ignition delay becomes slightly longer with the increases of biodiesel. The increase in physical delay could explain this. The ignition delay is the sum of the physical delay and the chemical delay. The increase in biodiesel content increases viscosity, thus reducing the atomization of droplets and volatility of GB blends. The bigger droplets decrease spray breakup, evaporation, and mixing; therefore, the physical delay increases. In contrast, the chemical delay decreases due to the highly flammable characteristic of biodiesel. The cumulative effect of the two factors increases the ignition delay after the biodiesel content continues to grow by over 60 % due to the dominance of physical delay. Besides, the ignition delay sharply decreases when the ambient temperature rises. It agrees with previous studies, which were carried out using diesel fuels and other alternative fuels.

3.2 Lift-off length results

Here will discuss the lift-off length parameter for the different blended fuel samples. Properties of liquid fuel, including viscosity, volatility, density, etc. play a crucial role in the lift-off length result. The natural soot luminous imaging technique was used to observe the effect of variations in GB blends on the lift-off length. Fig. 10 plots the measured lift-off length of the GB blends for different ambient temperatures (750 K, 800 K and, 900 K), 21 % oxygen content, and 10 kg/m^3 density. In general, the lift-off length significantly increased with increasing biodiesel concentration under gas temperature conditions as 800 K and 900 K. As the discussion above, although the gasoline fuel has the most extended ignition delay, it has the shortest lift-off of length. One reason for its shortest lift-off length is very low viscosity and surface tension. It can easily cause cavitation in the nozzle flow, resulting in a drop in the discharge coefficient of the nozzle and reduced flow characteristics. Another probable reason for the shorter lift-off length is the gasoline radial dispersion characteristics. The gasoline has high instability on the spray surface due to its low viscosity and surface tension characteristics, so spray development in the direction of the spray axis is slow, thus the shortest lift-off length. The increase in biodiesel ratio caused the rise of lift-off length. Because the higher biodiesel ration increases the viscosity and surface tension of the blended fuel, leading

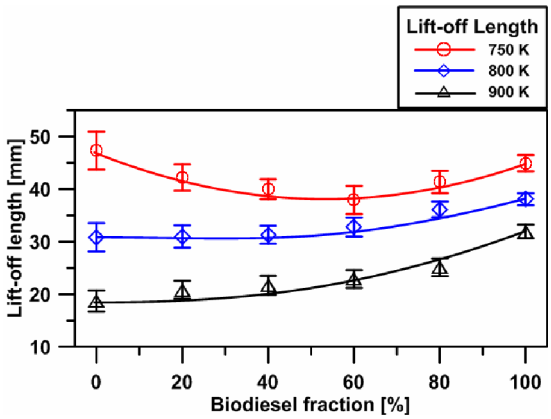

Fig. 10. Lift-off length under different temperature of 750 K, 800 K and 900 K temperature, 21 % oxygen content, and 10 kg/m^3 density.

to an increase of the size of fuel droplets and momentum in the fuel spray. Therefore, the combustion flame moves further downstream, and the lift-off length increases.

Differently, the lift-off length tends to decrease with increasing biodiesel concentration (less than 60 % biodiesel) at 750 K, 21 % oxygen content, and 10 kg/m^3 density. The differences observed between this and the cases mentioned above can be explained by the effect of biodiesel addition on the ignition delay. The significant decrease in ignition delay leads to reducing the time for movement of combustion flame at the downstream area, thus decreasing lift-off length. It is dominant in comparison to the increase lift-off length due to the increase in viscosity and surface tension. In this ratio range, the increase in biodiesel significantly reduces the chemical delay, which has the most powerful impact on the decrease of lift-off length. However, above 60 % biodiesel content, lift-off length trended to rise again like previous cases with the increase of biodiesel content. In this range, the increase of the ignition delay is a little bit with the rise of biodiesel content, so it is not a substantial impact on lift-off length. We note that increase in viscosity and surface tension are dominant in this case. The biodiesel fuel has high viscosity and high surface tension properties, so spray of the fuel blend with higher biodiesel content develops faster in the direction of the vertical axis. Also, high viscosity and surface tension, the fuel droplets become bigger size with higher momentum flux, hence the spray penetration of fuel blend with higher biodiesel content is accelerated in the direction of the vertical axis, resulting in the increase in lift-off length.

4. Conclusion

This study analyzed the effects of the different gasoline-biodiesel ratios on its ignition delay and lift-off length under low-temperature range using the constant volume combustion chamber. The ignition delay is obtained using two different methods: Pressure-based ignition delay and luminosity-based ignition delay. The natural soot luminous emission from combustion images was utilized to measure the lift-off length. Based on the experimental results, several main conclusions can be drawn as follows:

(1) The experimental results showed that the ignition delay presented similar trends for both pressure and luminous approaches. However, the pressure ignition delay is always a little longer than the luminous ignition delay. This difference can increase or decrease depending on the mixing process and the period of ignition delay. These results also agree with the previous researches and elucidated the effect of gasoline-biodiesel blend ratios on ignition delay, lift-off length, combustion phasing, and heat release rate.

(2) For below 60 % biodiesel, the GB blend with a higher biodiesel content reduced the chemical delay, leading to the advanced combustion phasing. The gasoline shows the maximum peak of HRR because of the extension of the mixing process that results in a more substantial mass of air-fuel mixture before the start of combustion. The 750 K case, biodiesel addition significantly advanced the combustion phasing; it confirmed its capacity to help the cold start and prevent the misfiring at low-engine load. However, over 60 % biodiesel ratio, the combustion phasing is not different so much.

(3) Generally, the ignition delay decreases with an increase in biodiesel content due to the higher cetane number. But for an ambient temperature of 900 K, the content of biodiesel is more top than 60 %; the ignition delay becomes slightly longer with the increases of biodiesel due to the significant rise in physical delay in total ignition delay.

(4) The lift-off length increased with an increase in biodiesel fraction under gas temperature conditions as 800 K and 900 K because of very high viscosity and surface tension of biodiesel. Differently, the lift-off length tends to decrease with the rise in biodiesel concentration (less than 60 % biodiesel) at 750 K case. Because the sharp reduction of ignition delay leads to reducing the time for movement of combustion flame at the downstream area, thus decreasing lift-off length.

(5) The evolution of the combustion frame for pure gasoline, GB20, GB40, GB60, GB80, and pure biodiesel were not similar during the combustion process. This phenomenon can be explained by the difference in cetane number, which reduces the chemical delay time while the different fuel properties change the size of fuel droplets, thus enhancing or hindering the air-fuel mixing process.

Acknowledgments

This research was financially supported by the CEFV (Center for Environmentally Friendly Vehicle) as Global-Top Project of KMOE (2016002070009, Development of Engine System and Adapting Vehicle for Model 110cc and 300cc Correspond to EUERO-5 Emission), and following are results of a study on the "Leaders in Industry-University Cooperation +" Project, supported by the Ministry of Education and National Research Foundation of Korea.

Nomenclature

GB : Gasoline-biodiesel
CVCC : Constant volume combustion chamber
GB20 : Gasoline-biodiesel blend with 20 % biodiesel
GB40 : Gasoline-biodiesel blend with 40 % biodiesel
GB60 : Gasoline-biodiesel blend with 60 % biodiesel
GB80 : Gasoline-biodiesel blend with 80 % biodiesel
CMOS : Complementary metal-oxide-semiconductor
HRR : Heat release rate
CI : Combustion ignition
NOx : Nitrogen oxide
THC : Total hydrocarbons
HC : Hydrocarbons
CO : Carbon monoxide
PM : Particulate matter
RCCI : Reactivity controlled compression ignition

HCCI : Homogeneous charge compression ignition mode
GCI : Gasoline compression ignition
EGR : Exhaust gas recirculation
ICCD : Intensified charge-coupled device
C_2H_2 : Acetylene
Ar : Argon
N_2 : Nitrogen
O_2 : Oxygen
RON : Research octane number
MON : Motor octane number
ECN : Engine combustion network

References

[1] R. Stone and J. K. Ball, *Automotive Engineering Fundamentals*, USA, Warrendale, PA 15090-001.

[2] J. B. Heywood, *Internal Combustion Engine Fundamentals*, New York, USA, McGraw-Hill Education (1988).

[3] W. W. Pulkrabek, *Engineering Fundamentals of the Internal Combustion Engine*, USA, Prentice Hall Upper Saddle River, New Jersy 07458.

[4] G. T. Kalghatgi, The outlook for fuels for internal combustion engines, *International Journal of Engine Research* (2014) 1-17.

[5] C. H. Muellller, A. L. Boehman and G. C. Martin, An experimental investigation of the origin of increased NOx emission when fueling a heavy-duty compression ignition engine with soy biodiesel, *SAE International* (2009) 2009-01-1792.

[6] R. Hanson, D. Splitter and R. Reitz, Operating a heavy-duty direct-injection compression-ignition engine with gasoline for low emissions, *SAE Technical Paper* (2019) 2009-01-1442.

[7] National Research Council, *Technologies and Approaches to Reducing the Fuel Consumption of Medium-and Heavy-duty Vehicles*, National Academies Press (2010).

[8] B. Yang, S. Li, Z. Zheng, M. Yao and W. Cheng, A comparative study on different dual-fuel combustion modes fuelled with gasoline and diesel, *SAE Technical Paper* (2012) 2012-01-0694.

[9] Y. Shi and R. D. Reitz, Optimization of a heavy-duty compression-ignition engine fueled with diesel and gasoline-like fuels, *Fuel,* 89 (2010) 3416-3430.

[10] D. Han, Y. Duan, C. Wang, H. Lin and Z. Huang, Experimental study on the two stage injection of diesel and gasoline blends on a common rail injection system, *Fuel,* 159 (2015) 470-475.

[11] W. J. Thoo, A. Kevric, H. K. Ng, S. Gan, P. Shayler and A. La Rocca, Characterisation of ignition delay period for a compression ignition engine operating on blended mixtures of diesel and gasoline, *Applied Thermal Engineering,* 66 (2014) 55-64.

[12] D. N. Vu, S. K. Das and O. Lim, Characteristics of auto-ignition in gasoline-biodiesel blended fuel under engine-like conditions, *IMechE (2018) Journal of Automobile Engineering* (2018) 1-13.

[13] R. Hanson, S. Curran, R. Wagner, S. Kokjohn, D. Splitter and R. Reitz, Piston bowl optimization for RCCI combustion in a light-duty multi-cylinder engine, *SAE International* (2012) 3012-01-0380.

[14] B. Yang, M. Yao, W. K. Cheng, Y. Li, Z. Zheng and S. Li, Experimental and numerical study on different dual-fuel combustion modes fuelled with gasoline and diesel, *Applied Energy* (2014) 722-733.

[15] S. Curran, V. Prikhodko, K. Cho, C. Sluder, J. Parks, R. Wagner, S. Kokhohn and R. D. Reitz, In-cylinder fuel blending of gasoline/diesel for improved efficiency and lowest possible emissions on a multi-cylinder light-duty diesel engine, *SAE International* (2010) 2010-01-2206.

[16] C. A. Adams, P. Loeper, R. Krieger, M. J. Andrie and D. E. Foster, Effects of biodiesel-gasoline blends on gasoline direct-injection compression ignition (GCI) combustion, *Fuel,* 111 (2013) 784-790.

[17] Y. Putrasari and O. Lim, A study on combustion and emission of GCI engines fueled with gasoline-biodiesel blends, *Fuel,* 189 (2017) 141-154.

[18] Y. Putrasari and O. Lim, A study of a GCI engine fueled with gasoline-biodiesel blends under pilot and main injection strategies, *Fuel,* 221 (2018) 269-282.

[19] J. Yeh, *An Alternative Energy Source*, COSMOS, UC Davis, Cluster 2 (2007).

[20] J. M. Marchetti and Z. Fang, *Biodiesel: Blends, Properties and Applications (Energy Science, Engineering and Technology)*, New York: Nova Science Publishers (2014).

[21] Z. Luo, M. Plomer, T. Lu, S. Som and D. E. Longman, Sarrathy SM, A reduced mechanism for biodiesel surrogates for compression ignition engine applications, *Fuel,* 99 (2012) 143-153.

[22] S. Kook, C. Bae, P. C. Miles, D. Choi and L. M. Pickett, The influence of charge dilution and injection timing on low temperature diesel combustion and emissions, *SAE Technical Paper* (2005) 2005-01-3837.

[23] J. Benajes, R. Payri, M. Bardi and P. Martí-Aldaraví, Experimental characterization of diesel ignition and lift-off length using a single-hole ECN injector, *Applied Thermal Engineering,* 58 (2013) 554-563.

[24] R. Payri, J. P. Viera, Y. Pei and S. Som, Experimental and numerical study of lift-off length and ignition delay of a two-component diesel surrogate, *Fuel,* 158 (2015) 957-967.

[25] S. K. Das, K. Kim and O. Lim, Experimental study on non-vaporizing spray characteristics of biodiesel-blended gasoline fuel in a constant volume chamber, *Fuel Processing Technology,* 178 (2018) 322-335.

[26] J. I. Ghojel and X.-T. Tran, Ignition characteristics of diesel - water emulsion sprays in a constant-volume vessel: Effect of injection pressure and water content, *Energy & Fuels,* 24 (2010) 3860-3866.

[27] Y. Ma, S. Huang, R. Huang, Y. Zhang and S. Xu, Ignition and combustion characteristics of n-pentanol-diesel blends in a constant volume chamber, *Applied Energy,* 185 (2017)

519-530.

[28] R. Payri, F. J. Salvador, J. Manin and A. Viera, Diesel ignition delay and lift-off length through different methodologies using a multi-hole injector, *Applied Energy,* 162 (2016) 541-550.

[29] M. Bardi, R. Payri, L. M. Malbec, G. Bruneaux, L. M. Pickett, J. Manin, T. Bazyn and C. Genzale, Engine combustion network: Comparison of spray development, vaporization, and combustion in different combustion vessels, *Atomization and Sprays,* 22 (2012) 807-842.

[30] C. Chartier, U. Aronsson, Ö. Andersson, R. Egnell and B. Johansson, Influence of jet-jet interactions on the lift-off length in an optical heavy-duty DI diesel engine, *Fuel,* 112 (2013) 311-318.

[31] D. L. Siebers and B. S. Higgins, Flame lift-off on direct-injection diesel sprays under quiescent conditions, *SAE Paper Series* (2001) 2001-01-0530.

[32] L. M. Pickett, S. Kook and T. C. Williams, Visualization of diesel spray penetration, cool-flame, ignition, high-temperature combustion, and soot formation using high-speed imaging, *SAE Paper* (2009) 2009-01-0658.

[33] K. Kalti and M. Mahjoub, Image segmentation by gaussian mixture models and modified FCM algorithm, *The International Arab Journal of Information Technology,* 11 (1) January (2014).

[34] B. Obara, Identification of transcrystalline microcracks observed in microscope images of a dolomite structure using image analysis methods based on linear structuring element processing, *Computers & Geosciences,* 33 (2007) 151-158.

[35] S. J. Chapman, *MATLAB Programming for Engineers*, Toronto, Canada: RPK Editorial Services (2008).

[36] M. Adam, *Ignition Delay of JP-8 at Diesel Engine Conditions*, University of Wisconsin-Madison (2011).

[37] M. Malin, V. Krivopolianskii, B. Rygh, V. Aesoy and E. Pedersen, Soot investigation on fish oil spray combustion in a constant volume cell, *SAE International* (2015) 2015-24-2479.

[38] S. Huang, P. Deng, R. Huang and Z. Wang, Visualization research on spray atomization, evaporation and combustion processes of ethanol-diesel blend under LTC conditions, *Energy Conversion and Management,* 106 (2015) 911-920.

Ocktaeck Lim received his B.S. and M.S. degrees in Mechanical Engineering from Chonnam National University, Korea, in 1998 and 2002, respectively. He then received his Ph.D. degree from Keio University in 2006. Dr. Lim is currently a Professor at the School of Automotive and Mechanical Engineering at University of Ulsan in Ulsan, Korea. Dr. Lim's research interests include Internal Combustion Engines, Alternative Fuel and Thermodynamics.